# Spectral filters in quantum mechanics: A measurement theory perspective

Amrendra Vijay and Robert E. Wyatt
*Institute for Theoretical Chemistry, Department of Chemistry and Biochemistry, The University of Texas at Austin, Austin, Texas 78712-1167*
(Received 28 February 2000)

We present the time-domain theory of spectral filters, starting with the basic propositions of the theory of measurement in quantum mechanics, and develop its parameter-free implementation in the traditional correlation function as well as the filter diagonalization (FD) form. The present study unifies all the time-domain spectral filter algorithms in the literature, under a single theme which is based on the notion of selective measurements. For specific numerical purposes, we have selected Chebyshev polynomials for developing the time propagator and this permits us to carry out the relevent time integrals fully analytically and obtain FD equations in a numerically convenient form. We also argue that the FD method is a particular realization of the general spectral filter goal and it is constrained, in general, by the time-energy uncertainty regime at least as much as the correlation-function-based method. To contrast the performance of the correlation function and the FD methods, we have carried out the detailed numerical experiments on a model system, which suggest that the FD method needs almost as much time propagation as the correlation function method, in order to identify the correct spectrum. The difference lies in the procedure for the exact location of eigenvalue positions, for which the FD method employs a diagonalization step while the correlation function method involves the location of zeros.

PACS number(s): 02.70.−c, 02.60.Lj, 02.60.Ed, 03.65.Ge

## I. INTRODUCTION

The quantum description of physical and chemical processes frequently demands an accurate knowledge of the eigenspectrum of the corresponding system Hamiltonian. The conventional noniterative matrix diagonalization techniques are not suitable for this purpose, as most chemical and physical systems of interest involve a large rank Hamiltonian. However, iterative diagonalization methods (e.g., the Lanczos reduction technique) have been successfully used over the years. On the other hand, we frequently seek eigenvalues and eigenvectors only within a relatively small spectral window, such as those near the transition state or those near the energy of the local mode overtones. The realization that it may be possible to extract a small window from any region of the spectrum of the Hamiltonian, using a *spectral filter*, without solving the eigenvalue problem completely, has witnessed a tremendous upsurge of interest in recent years [1–34]. In general, spectral filter theory may be broadly classified into two complementary streams, such as those involving time-independent and time-dependent approaches. In this context, as the eigenvalue problem is intrinsically a time-independent issue in quantum mechanics, Wyatt has proposed the use of the time-independent Green function in conjunction with the traditional Lanczos reduction technique (GFLA) to extract the eigenvalue information near the test energy [30–33]. On the other hand, the advent of time-domain theory of spectral filters is due to an important realization that ''an arbitrary initial state (assumed not to be orthogonal to any eigenstate of the system), after evolving under the action of the Hamiltonian for a *relatively short time*, projects into the space spanned by the energies close to the test energy, and various propagated wavepackets at different energies within a window serve as a basis for conventional matrix diagonalization, yielding thereby the spectrum belonging to the chosen window.'' This appealing proposition was apparently first implemented for practical calculations by Heller and co-workers [1,2] within the semiclassical framework. This method, through the innovation of Neuhauser [3–6], has come to be known as the *filter diagonalization* (FD) method. The FD method originally utilized the exact quantum evolution of the system and later it was also recast in terms of the discrete time-dependent correlation function [6,19]. The FD method has been argued to be valid, even when the dynamics underlying the correlation function is not quantum mechanical [6]. We note that various formulations of the original FD proposition [3], aside from the implementation strategy, fundamentally differentiate only in the choice of *damping functions*. Of the damping functions, the *Gaussian* type has been frequently utilized, though a more elaborate choice of damping functions has also been made [6,27]. The FD method utilizes the *spectral density operator* (SDO) as the filter operator. The SDO has also been utilized by Kouri, Hoffman, and co-workers [11–13] for implementation of the continuous correlation-function-based spectral method.

In this paper, we will be concerned with the fundamental properties of the SDO. The time-domain theory of spectral filters based on the above proposition has been contrasted with the traditional correlation-function-based time-dependent spectral method [35] and it has been qualitatively argued that the time-domain spectral filter theory can bypass the time-energy uncertainty constraint, and hence it is superior in numerical performance [5,20]. We parenthetically note that the time-energy uncertainty principle dictates the minimum time one has to propagate the wave packet in order to recover the eigenspectrum of the system Hamiltonian faithfully, and this is also frequently known as the *sampling theorem* [36] in communication problems. Whether the FD method can bypass the uncertainty constraint is a fundamen-

 

tal issue, and this will be examined here in analytical as well as numerical terms.

In this paper, we develop the time-domain theory of spectral filters from the *measurement* perspective [37–39] and advance arguments that the FD method is a particular implementation of the general spectral filter goal. The measurement perspective gives rise to a unified understanding of various time-domain filter algorithms known in the literature and also clarifies the central issue of the role of the time-energy uncertainty principle. For illustration, we have implemented a parameter (arbitrary) free realization of the filter paradigm into the traditional continuous correlation function as well as the FD form, and compare their numerical performance in detail.

The organization of this paper is as follows. In Sec. II, we elaborate on the concept of spectral filters from the measurement perspective in quantum mechanics, followed by various approximations to the general filter operator and its representation in the orthogonal polynomial form. Implementation of the filter paradigm in the form of a correlation function as well as FD is presented in Sec. III. We discuss the details of the model system studied here in Sec. IV, and in Sec. V we present the computational results. We conclude the presentation in Sec. VI.

## II. THEORY

In what follows, we discuss the basic physics underlying the spectral filter concept, and outline the protocol based both on the traditional time correlation function and the filter diagonalization (FD) method. In order to facilitate an even and consistent comparison, we will adopt the Chebyshev polynomials as the basic time propagation system [40] and rely on our ability to carry out the time-energy Fourier transformation fully analytically, without recourse to any damping function. The choice of Chebyshev polynomials is due to their extraordinary analytical properties, not shared by other classical orthogonal sets, and this eventually leads to a very compact and numerically efficient formulation of the continuous-time FD method.

### A. Selective measurements and spectral filters

The theory of spectral filters can be viewed as originating from the basic propositions of the theory of measurement in quantum mechanics [37–39]—an integral part of the Copenhagen doctrine, as elaborated in the classic treatise of Dirac [37]. It will become clear later that the concept of ''filter'' has a direct connotation with the act of measurement. In the following, we state the basic assumptions underlying the theory of measurement [37].

(i) An act of measurement always causes the quantum system to jump into an eigenstate of the corresponding real dynamical variable (for example, the Hamiltonian of the system) that is being measured; that is, any result of a measurement of a real dynamical variable is one of its eigenvalues. Conversely, every eigenvalue is a possible result of measurement of the dynamical variable for some state of the quantum system.

(ii) If a certain real dynamical variable is measured with a system in an arbitrary state, the states into which the system may jump on account of the measurement are such that the original arbitrary state is dependent on them. Since the states into which the system may jump are all eigenstates, an arbitrary state is dependent on the eigenstates of the real dynamical variable.

These are *constructive* propositions and they provide algorithmic clues as to how the theory of spectral filters has to be built in quantum mechanics. We will also utilize the fact that eigenstates of the system Hamiltonian form an orthogonal set, but we will not assume the existence of the time-dependent Schrödinger equation (TDSE). We first point out the meaning of the second assumption. It empowers us to analyze the initial arbitrary state in an orthogonal reference space spanned by the eigenvectors $|\phi(x,\epsilon_m)\rangle$ of the system Hamiltonian. Without loss of generality, we assume the reference space to be of finite dimension. Thus we can write an arbitrary initial state (in the energy representation) as follows:

$$|\psi(x,0)\rangle=\sum_m A(\epsilon_m)|\phi(x,\epsilon_m)\rangle, \tag{1}$$

where $A_m=\langle\phi(x,\epsilon_m)|\psi(x,0)\rangle$ is the weight with which the $m$th eigenstate contributes to the initial wave packet. Thus the second assumption allows us to consider the initial arbitrary state to be synthesized from the eigenstates of the system. In order to extract the spectral information from $|\psi(x,0)\rangle$, we resort to the first measurement assumption. To clarify the meaning of measurement, we introduce the notion of *selective measurement* or *filtration*, in which we imagine a process that, when applied to $|\psi(x,0)\rangle$, selects only one of the eigenstates and rejects all others [38,39]. In other words,

$$|\psi(x,0)\rangle \quad \overset{a\ measurement}{- - - - - \longrightarrow} \quad |\phi(x,\epsilon_m)\rangle \tag{2}$$

Thus a measurement always changes the state, the only exception being when the state itself is one of the eigenstates of the real dynamical variable (the Hamiltonian, in the present context), in which case the measurement does not change the state. Mathematically, such a *selective measurement* amounts to applying a projection operator, $\hat{\Lambda}(\epsilon_m)$. The application of a projection operator on $|\psi(x,0)\rangle$ selects the eigenstate, as is clear from the following implicit definition:

$$\begin{aligned}\hat{\Lambda}(\epsilon_m)|\psi(x,0)\rangle&=\{|\phi(x,\epsilon_m)\rangle\langle\phi(x,\epsilon_m)|\}|\psi(x,0)\rangle\\&=|A(\epsilon_m)|\phi(x,\epsilon_m)\rangle.\end{aligned} \tag{3}$$

The measurement paradigm can also be applied to the correlation function,

$$\begin{aligned}\hat{\Lambda}(\epsilon_m)\rho(0)&=\langle\psi(x,0)|\{|\phi(x,\epsilon_m)\rangle\langle\phi(x,\epsilon_m)|\}|\psi(x,0)\rangle\\&=|A(\epsilon_m)|^2.\end{aligned} \tag{4}$$

Thus the projection operator acting on the correlation function, which is unity at zero time, filters the corresponding spectral intensity and this also provides a valid avenue for spectral analysis.

Having established the concept of *filter* through the notion of *selective measurement*, we now need to formulate an explicit and operational definition of the projection operator. We note that Eqs. (3) and (4) provide only a *nonconstructive*

assertion to this end. By ''nonconstructive'' we mean that the proposition is devoid of any practical value, but its nonexistence would lead to a logical contradiction. As we are dealing with the energy eigenstates, it is obvious that a projection operator of the type $\delta(E-\hat{\mathcal{H}})$, where $\hat{\mathcal{H}}$ is the Hamiltonian of the system and $E$ is the energy at which the filter operator is being applied, clearly satisfies the primary notion of the *selective measurement* and hence this would be a natural choice for the spectral analysis of the quantum system. In this way, we see that the entire spectral filter problem essentially reduces to finding an appropriate representation of the delta operator, $\delta(E-\hat{\mathcal{H}})$.

We note that the above notion of *selective measurement* has been popular in interpretative quantum mechanics and in fact Schwinger developed a formalism of quantum mechanics and introduced a measurement symbol $\mathbf{M}(\epsilon_m)$ and the correponding measurement algebra [38]. Schwinger's measurement symbol is identical to our elementary projection operator, $\hat{\Lambda}(\epsilon_m)$.

### B. Derivation of filters

Having recognized $\delta(E-\hat{\mathcal{H}})$ as the basic object underlying the spectral filter goal, we now focus upon its practical representation. In the following discussion, we also advance the reasoning leading to $\delta(E-\hat{\mathcal{H}})$ as the basis for various FD methods and we will contrast this with the correlation function approach. We note that the delta operator $\delta(E-\hat{\mathcal{H}})$ is identical to the *spectral density operator* (SDO) known through the work of Kouri and co-workers [11–13]. This operator refers to the *selective measurement* process here and we know that no measurement is, in general, operationally perfect [imperfection here lies in the construction of the measuring apparatus, $\delta(E-\hat{\mathcal{H}})$, and has nothing to do with the uncertainty principle] and hence $\delta(E-\hat{\mathcal{H}})$ can, in practical realization, at best represent a certain limiting process. That means that the application of $\delta(E-\hat{\mathcal{H}})$ ''forces'' the initial arbitrary state to jump into the vicinity of the energy eigenstate, $\phi(x,\epsilon_m)$, with ever-decreasing error, $(E-\epsilon_m)$, in the norm. There are several functions which, in specific limits, mimick the behavior of the $\delta$ function, and the typical examples are $1/2\zeta\exp(-|E-\hat{\mathcal{H}}|/\zeta)$, $(1/\pi)\zeta/[(E-\hat{\mathcal{H}})^2+\zeta^2]$, $1/\zeta\sqrt{\pi}\exp[-(E-\hat{\mathcal{H}})^2/\zeta^2]$, and $1/\pi\zeta\,\mathrm{sinc}([E-\hat{\mathcal{H}}]/\zeta)$ [where $\mathrm{sinc}(x)=\sin(x)/x$], in the limit $\zeta\to 0$, and any of these approximations could be utilized to derive equations for the spectral filter. We notice that the parameter $\zeta$ in all these approximations of $\delta(E-\hat{\mathcal{H}})$ is merely the inverse of the *physical time*, $T$ (this is implied from dimensional considerations), as time and energy are conjugate variables in quantum mechanics, and therefore the ''selective measurement'' demands the measurement process to be of ''infinite'' duration, which in the present context essentially means a continuous ever-ending limiting sequence. That is, as long as the measurement process is ''on,'' we can reach the eigenstate as close as we wish. The conjugacy of time and energy also suggests that the Fourier integral theorem [41] could be applied here in order to obtain an integral representation of the approximation of the $\delta$ operator. We thus write

$$\delta(E-\hat{\mathcal{H}})=\int_{-\infty}^{\infty}dt\,e^{i(E-\hat{\mathcal{H}})t}\times[\text{Fourier transformation of }\delta(E-\hat{\mathcal{H}})]. \tag{5}$$

Equation (5) is an identity of fundamental importance, as this enables us to obtain various spectral filters of our choice. In Eq. (5), we have implicitly assumed that the argument of the $\delta$ operator does not have any time dependence, and this is consistent with the fact that the eigenstate of the system is a time-independent concept. Now, as a definite example, let us consider $1/\zeta\sqrt{\pi}\exp[-(E-\hat{\mathcal{H}})^2/\zeta^2]$ and $1/\pi\zeta\,\mathrm{sinc}([E-\hat{\mathcal{H}}]/\zeta)$ as approximations to $\delta(E-\hat{\mathcal{H}})$, the Fourier pairs of which are $1/2\pi$ for $|t|<T$ and $\sqrt{1/2\pi}\exp(-t^2/4T^2)$ for $T>0$, respectively, and thus we obtain from Eq. (5),

$$\delta^{\text{approx}}(E-\hat{\mathcal{H}})=\frac{1}{\sqrt{2T}}\int_{-T}^{T}dt\,e^{iEt}e^{-i\hat{\mathcal{H}}t}=\frac{1}{\sqrt{2\pi}}\int_{-\infty}^{\infty}dt\,e^{iEt}e^{-i\hat{\mathcal{H}}t}\quad(\text{in the limit } T\to\infty), \tag{6}$$

$$\delta_G^{\text{approx}}(E-\hat{\mathcal{H}})=\frac{1}{\sqrt{2T}}\int_{-T}^{T}dt\,e^{iEt}e^{-i\hat{\mathcal{H}}t}e^{-t^2/4T^2}. \tag{7}$$

Equation (6) states that filteration can be accomplished by the Fourier transformation of an arbitrary state, evolved under $e^{-i\hat{\mathcal{H}}t}$, which is consistent with the time-dependent Schrödinger equation. Noticeably, we have arrived at Eq. (6) with just the logical extension of the two measurement assumptions. Equation (7), on the other hand, represents the Fourier transformation with Gaussian damping. If we use $(1/\pi)\zeta/[(E-\hat{\mathcal{H}})^2+\zeta^2]$ as the approximation of the $\delta$ operator, we would obtain the Fourier transformation with exponential damping, $e^{-\zeta|t|}$. As such, Eq. (6) and its variants like Eq. (7) have been the starting point for various FD methods [3,6,12,18,23]. We note that the application of Eq. (6) in the FD context is known as a ''box filter,'' otherwise the filter is known with the corresponding damping function. It is now apparent that only the sinc function, contrary to other approximations, gives rise to the simplest integral representation to the $\delta$ operator, which does not involve any arbitrary damping function, and therefore this has to be the most natural choice as the physical theory cannot be dependent on some arbitrary parameter. In practice, however, the application of a suitable damping function may be advantageous for specific purposes. We will elaborate upon this point later on. Now, as time is operationally taken as a continuous variable, the integrand in Eq. (6) is a continuous function of time, and the range of this function goes, in principle, to infinity. Therefore, Eq. (6) is an instance of Fourier transformation of the function on the full line $(-\infty,+\infty)$, the consequence of which is that $\delta^{\text{approx}}(E-\hat{\mathcal{H}})$ is also, in principle, continuous. That is, the individual Fourier components in Eq. (6), $E_k=(2\pi/T)k$, where $k$ is an integer, can be brought, in the

limit $T\rightarrow\infty$, as close as we wish. In this limit, a specific functional value, $\delta^{\text{approx}}(E_k-\hat{\mathcal{H}})$, cannot be correlated anymore to a definite Fourier component, but it has to be considered as a *spectral density*, and thus $\delta^{\text{approx}}(E-\hat{\mathcal{H}})$ represents the *spectral density operator* [41]. The significance of the Fourier integral theorem is that we can resolve an arbitrary function in the time domain, $f(t)$, into its harmonic components, by constructing the continuous function $\delta^{\text{approx}}(E-\hat{\mathcal{H}})$, which represents a spectral density. We point out that the range of integration in Eqs. (6) and (7) (i.e., from $-T$ to $T$, with limit $T\rightarrow\infty$) assumes the validity of time-reversal symmetry, which is fully justified for the eigenvalue problems in quantum mechanics. In fact, the imposition of time-reversal symmetry in quantum mechanics essentially amounts to a definite choice of the *phase factor*, which can conveniently be taken as unity for eigenvalue problems [42].

We now discuss the role of damping functions containing an arbitrary parameter, as manifested in Eq. (7). We have already recognized Eq. (6), which is a Fourier series, as the statement of the TDSE and therefore we need to understand the situations in which the use of the damping function is needed for the convergence of the series. The following argument is based on the studies of Lanczos [41]. Ordinarily, a Fourier series means that we sum up an increasing number of terms of the series by constantly adding one more term to the previous terms, and if the sum uniformally converges, then the coefficients of the series cannot be anything but the usual Fourier coefficients as obtained by a definite integral. On the other hand, if the function domain includes some singular point and the convergence is no longer uniform (an example being the appearance of the so-called Gibb's phenomenon [41]), the overall convergence of the series may be enhanced by adjusting the Fourier coefficients using certain suitable weight factors, which change as we go along the series (damping function). It should, however, be noted that if the function is in fact exactly equal to the sum of a finite number of (say $N$) Fourier terms, then the ordinary way of summing the series (that is, without using the damping function) will recover the function exactly after $N$ terms, while the use of the damping function will *never* get the function exactly, unless $N$ increases to infinity. Thus, every approximation of the $\delta$ operator, which involves an arbitrary damping parameter, is generally a legitimate analytical proposition, in the sense that in convergence proofs we are only interested in what eventually happens to the series and we do not care how many terms are needed for a certain accuracy. In practice, however, different approximations of the $\delta$ operator, owing to the presence of an arbitrary damping parameter, will exhibit qualitatively different numerical behavior. The use of damping functions in the filter context should be seen in this light.

Now, a remark on the so-called *time-energy uncertainty principle* [43] is in order. It is clear that the time integration in Eq. (6) can, in practical applications, be carried out only for a finite interval (say, $-T/2$ to $+T/2$), and this sets a limit on the energy resolution (maximum $2\pi/T$) during spectral analysis while using Eq. (6) or Eq. (7). This fact, obvious from the Fourier integral theorem, is variously known as the *time-energy uncertainty principle* or the *sampling theorem* [36]. It must be emphasized that the use of a damping function [as in Eq. (7), for example] does not, in any way, let us bypass this uncertainty constraint. This point will be further considered in the development of the FD method.

We will now discuss the issues related to the implementation of Eq. (6). In principle, one could use any short-time propagator to generate the integrand in Eq. (6) at discrete times and carry out the integration numerically. However, the numerical integration is frought with difficulties as one has to take cognizance of the *sampling theorem* [36]. That is, the sampling interval $\Delta t$ has to be less than at least $2\pi/E$, where $E=E_{\max}-E_{\min}$ is the total spectral range contained in the Hamiltonian. As Eq. (6) involves an integration over time, it would be very convenient to utilize a propagation method that splits the evolution operator $e^{-i\hat{\mathcal{H}}t}$ into a Hamiltonian part and a time part, so that one can attempt to carry out the time integral in Eq. (6) or its variants like Eq. (7) fully analytically. In this context, a classical orthogonal polynomial-based recursive propagation method is an ideal choice. The choice of the orthogonal polynomial and the approximation of the $\delta$ operator would be largely dictated by our ability to carry out the time integral fully analytically, otherwise the ensuing numerical scheme would turn out to be numerically less efficient and transparent [34]. In the following, we consider the Chebyshev polynomial-based representation of the evolution operator [40], in conjunction with Eq. (6). Thus we can write

$$e^{-i\hat{\mathcal{H}}t}=\sum_{m=0}^{N\rightarrow\infty}(2-\delta_{m0})(-i)^m e^{-i\bar{\lambda}t}J_m(t\Delta\lambda)T_m\left(\frac{\hat{\mathcal{H}}-\bar{\lambda}}{\Delta\lambda}\right), \tag{8}$$

where $\bar{\lambda}$ and $\Delta\lambda$ are the scaling parameters to adjust the range of the Hamiltonian, $\hat{\mathcal{H}}$, to fall in the interval $-1$ to $+1$, as demanded by the definition of the Chebyshev polynomial. Now we substitute Eq. (8) into Eq. (6) and carry out the time integral from 0 to $T$ (with $T\rightarrow\infty$) to obtain the following expression for the approximate $\delta$ operator:

$$\delta^{\text{approx}}(E-\hat{\mathcal{H}})=\frac{2}{\Delta\lambda}(1-\bar{E})^{-1/2}\sum_{m=0}^{N}(2-\delta_{m0})\times[T_m(\bar{E})-iV_m(\bar{E})]T_m(\bar{H}), \tag{9}$$

which, on the application of time-reversal symmetry, yields

$$\delta^{\text{approx}}(E-\hat{\mathcal{H}})=\frac{2}{\Delta\lambda}(1-\bar{E})^{-1/2}\times\sum_{m=0}^{N}(2-\delta_{m0})T_m(\bar{E})T_m(\bar{H}). \tag{10}$$

Here $\bar{E}$ and $\bar{H}$ are the normalized energy and Hamiltonian, respectively. $T_m(\bar{E})$ and $V_m(\bar{E})$ refer to the two linearly independent solutions of the second-order differential equation, which Chebyshev polynomials of type I satisfy, and of which only $T_m$ is a polynomial. We note that Eq. (7) cannot be integrated fully analytically with Eq. (8) and hence it would not be possible to get a closed-form expression for the Gaussian approximation for $\delta(E-\hat{\mathcal{H}})$ as in Eqs. (9) and

(10). It is clear from Eq. (9) that the polynomial feature is lost in the absence of the time-reversal symmetry.

## III. IMPLEMENTATION

In this section, we discuss the continuous-time implementation of spectral filters for correlation functions as well as FD, and for this purpose we will utilize the sinc function approximation to the projection operator [cf., Eq. (6)]. The continuous-time formulation is generally sufficient for bound-state problems. However, it turns out that if we restrict the time integral only from 0 to $T$ (with $T\rightarrow\infty$), the discrete time implementation of the FD method may be useful [19] and therefore we will also address this issue.

### A. Correlation function

Using Eqs. (4) and (10), we obtain

$$\rho(E)=\frac{4}{\Delta\lambda}(1-\overline{E})^{-1/2}\sum_{m=0}^{N}\left(1-\frac{\delta_{m0}}{2}\right)T_m(\overline{E})U_m, \quad (11)$$

where $U_m=\langle\psi(x,0)|T_m(\overline{H})|\psi(x,0)\rangle$. Here $\rho(E)$ is a continuous function of energy and this function, in the limit $N\rightarrow\infty$, has a ''$\delta$-comb'' structure with different peaks located at $E=\epsilon_m$ (where $\epsilon_m$ is the $m$th eigenvalue) and $\rho(E)$ itself equals the spectral intensity, $|A(\epsilon_m)|^2$. We note that $\rho(E)$, for finite $N$, will have the sinc function type structure. We thus see that in the continuous correlation function method, we directly filter the spectral intensity, and the energy location of the eigenstate is essentially a side product. In practical calculations, one has to evaluate $U_m$ only once and store it. We can then, within a given energy window, sweep the function $\rho(E)$ to locate the energy position of the eigenstates. The energy interval $\Delta E$ at which one calculates $\rho(E)$ should be such that one does not miss any eigenstate, which means $\Delta E$ should be smaller than the expected smallest eigenvalue gap in the given energy window. The question now is, how many terms, $N$ in Eq. (11), should we retain so that we can faithfully identify all the eigenstates in a given energy window? The number $N$ essentially reflects the total length $T$ of the time propagation in Eq. (6), and this has to be larger than $T\Delta\lambda$, as is evident from Eq. (8). And the total length of the time propgation itself has to satisfy the time-energy uncertainty principle; that is, $T$ has to be greater than $2\pi/\Delta\epsilon$, where $\Delta\epsilon$ is the minimum eigenvalue gap within the given energy window. In practical realization, however, we can adopt a more pragmatic approach. We know that the function $\rho(E)$ will have maxima at the eigenvalue locations, along with the adjoining sinc structures which have continuously diminishing amplitudes as $N$ grows to infinity. We can then compute the first and second derivatives of $\rho(E)$ with respect to energy and superimpose this over $\rho(E)$. The eigenvalue locations are identified as the points where the first derivative passes through zero. In actual calculations, one may use other methods, such as the Newton-Raphson method [44], to locate the roots of $\partial\rho(E)/\partial E$. The required derivative expressions are as given below,

$$\frac{\partial\rho(E)}{\partial E}=\frac{4}{(\Delta\lambda)^2}(1-\overline{E})^{-3/2}\sum_{m=0}^{N}\left(1-\frac{\delta_{m0}}{2}\right)\times[mT_{m-1}(\overline{E})-(m-1)\overline{E}T_m(\overline{E})]U_m, \quad (12)$$

$$\frac{\partial^2\rho(E)}{\partial E^2}=\frac{4}{(\Delta\lambda)^3}(1-\overline{E})^{-5/2}\sum_{m=0}^{N}\left(1-\frac{\delta_{m0}}{2}\right)[3m\overline{E}T_{m-1}(\overline{E})+(m-1)\{(m-2)\overline{E}^2-(m+1)\}T_m(\overline{E})]U_m. \quad (13)$$

We note that Eqs. (12) and (13) have been obtained by differentiating a sort of ''discontinuous'' function $\rho(E)$ (in the limit $N\rightarrow\infty$), and hence their values will grow to ''infinity'' as $N$ becomes large. However, for the purpose of location of zeros, we can always scale Eqs. (12) and (13) arbitrarily down, as we are not concerned with their actual large values. We also point out that Eq. (11) is not properly normalized and it should be normalized with the factor $1/\sqrt{2T}$ for the determination of spectral intensity, $|A(\epsilon_m)|^2$, where the total propagation time $T$ can be estimated by the fact that $N$ is greater than $T\Delta\lambda$, where $N$ is the total number of terms required in Eq. (10) to obtain the well-resolved spectral features of the Hamiltonian.

### B. Filter diagonalization

The FD method is a practical realization of the *selective measurement* paradigm, and Eq. (6) or its variants like Eq. (7) in conjunction with Eq. (3) serves as the starting point. Using Eqs. (3) and (6), we write

$$\begin{aligned}|\chi(x,E)\rangle&=\hat{\Lambda}(E)|\psi(x,0)\rangle\\&=\left\{\lim_{T\rightarrow\infty}\int_{-T}^{T}dt\,e^{iEt}e^{-i\hat{\mathcal{H}}t}\right\}|\psi(x,0)\rangle\\&=\lim_{T\rightarrow\infty}\int_{-T}^{T}dt\,e^{iEt}|\psi(x,t)\rangle.\end{aligned} \quad (14)$$

Equation (14) is not properly normalized and we will discuss this issue later. In Eq. (14), we recognize $|\psi(x,t)\rangle$ as the time-evolved state and the time evolution itself is affected by the operator $e^{-i\hat{\mathcal{H}}t}$. Also, $E$ as well as $\hat{\mathcal{H}}$ is independent of time, in order to be consistent with Eq. (5). In this way, we recover the time-dependent Schrödinger equation, just with the logical extension of the measurement propositions. Now, Eq. (14) essentially states that the energy state $|\chi(x,E)\rangle$ can be extracted from the time evolution of an arbitrary state by utilizing the Fourier integral theorem. The crux of the FD method lies in an important observation that the integrand in Eq. (14) is highly oscillatory, and therefore reflects the possibility of strong cancellation for a moderately large value of $t$. As time goes on, we expect smaller contributions from the energy components away from $E$. This phenomenon is sometimes known as the *loss of phase coherence*, the result of which leads to the FD proposition [1–3] ''after a relatively short time the filtered state $|\chi(x,E)\rangle$ will span the space of

quantum states with energies close to $E$, and several such filtered states at a discrete set of energies within a given window can be used as a basis set to obtain the eigenvalues within the window, by conventional matrix diagonalization.'' In this sense, the time propagation step in the FD method acts as a *preconditioner* of the basis for eventual disentanglement of eigenstates by the diagonalization process. The filtered states $|\chi(x,E)\rangle$ are not expected to form an orthogonal set and, in practical applications, one has to make sure that the set is overcomplete, that is, the size of the matrix ($L$) we diagonalize is larger than the number of eigenvalues within the given window. Thus we express the energy eigenstate $|\phi(x,\epsilon_m)\rangle$ in terms of filtered states,

$$|\phi(x,\epsilon_m)\rangle = \sum_{l=1}^{L} B_{lm}|\chi(x,E_l)\rangle, \tag{15}$$

and obtain the eigenvalue problem in the matrix form as $\mathcal{HB}=\mathcal{SB}\epsilon$. Here $\epsilon$ is a diagonal matrix containing the eigenvalues, and the Hamiltonian and overlap matrices are defined, respectively, as follows:

$$S_{m,m'} = \langle \chi(x,E_m)|\chi(x,E_{m'})\rangle_x, \tag{16}$$

$$\mathcal{H}_{m,m'} = \langle \chi(x,E_m)|\hat{\mathcal{H}}|\chi(x,E_{m'})\rangle_x. \tag{17}$$

In this overcomplete eigensystem, the overlap matrix $S$ is generally singular and therefore we can use, for example, singular value decomposition (SVD) [45] for this purpose.

Eigenvalues obtained by the FD method may not all be true eigenvalues of the system, and therefore it is mandatory to carry out an independent check to differentiate the spurious eigenvalues from the true ones. To this end, the magnitude of the vector, $(\hat{\mathcal{H}}-\epsilon_m)|\phi(x,\epsilon_m)\rangle$, can be used as a parameter to serve the accuracy of the computed results. To be specific, we can compute the error norm $\Delta\epsilon_m$ defined as follows [6]:

$$\begin{aligned}(\Delta\epsilon_m)^2 &= |\langle \phi(x,\epsilon_m)|(\hat{\mathcal{H}}-\epsilon_m)^2|\phi(x,\epsilon_m)\rangle| \\ &= |(B^tH^2B)_{mm} - \epsilon_m^2(B^tSB)_{mm}|.\end{aligned} \tag{18}$$

Here, the $H^2$ matrix is defined as follows:

$$H^2_{mm'} = \langle x(x,\epsilon_m)|\hat{\mathcal{H}}^2|x(x,\epsilon_{m'})\rangle. \tag{19}$$

It has been shown that $(\Delta\epsilon_m)^2$ represents the upper bound on the true error of the eigenvalues [46]. For the purpose of error estimation, one may also use different variational principles, as suggested by Beck and Meyer [27].

The above discussion essentially completes the basic ideas involved in the FD method. Here, Eqs. (14)–(19) form the basic structure of the FD method, and the obvious question that remains is as how efficiently can we cast the working equations for the matrix elements [Eqs. (16) and (17)]. It is this stage that different strategies have been put forth in the literature [6,18,19,25,27,34]. In the present study, we utilize Eq. (10) for the projection operator as required in Eq. (14). A derivation of the overlap, Hamiltonian, and error matrix elements is presented in Appendix A.

Thus we see that the FD proposition offers an appealing viewpoint, and in this context the most important question now is how much time one has to propagate an initial arbitrary state in Eq. (14) for a faithful identification of all the eigenvalues in the window, and does the method really allow one to bypass the uncertainty principle. The FD proposition, as outlined above, does not make any such assertion to this end, and therefore we will reconsider Eq. (14). In fact, we arrived at Eq. (14) through the logical extension of the measurement notion, and therefore, in the limit $T\to\infty$, this only asserts ''either we filter the eigenstates or we do not.'' The limiting process in Eq. (14) is expected to be bounded by the time-energy uncertainty principle for a faithful filteration of eigenstates, and this is merely the assertion of the Fourier integral theorem. It is clear that if we do not exhaust the limiting process in Eq. (14), we once again filter some arbitrary states and these states may have nonzero spectral intensities only for the limited eigenstates close to the filter energy. However, no sweeping analytical assertion can be made as to whether states thus obtained are sufficient for the faithful identification of all the eigenvalues in the window by the diagonalization process. This issue is better settled by systematic numerical experiments.

So far the discussion was restricted to bound-state problems for which the imposition of time-reversal symmetry is legitimate, and we utilized the continuous-time formulation within the framework of Chebyshev polynomials. If we restrict the time integration only from 0 to $T$ (with $T\to\infty$), the $\delta$ operator will contain a nonpolynomial term, $V_m$ [cf., Eq. (9)], and the resulting overlap and Hamiltonian matrices will clearly be complex symmetric with complex eigenvalues—a situation typically encountered for the resonance problems by the complex scaling method. In this situation, it will not be possible to carry out partial summation of the double series by the method of a *Cauchy-like expansion* [47] as we have done in Appendix A, and therefore the resulting expressions for the overlap and the Hamiltonian matrices will no longer be in ''numerically friendly'' form. As shown in Ref. [19], it turns out that the discrete time implementation of the FD method in this case may be preferred as it allows a compact set of final equations for numerical purposes. This is described in Appendix B. In any case, we have to bear in mind that the discrete time sampling has to satisfy the sampling theorem [36]; that is, the time interval has to be less than $2\pi/\Delta\epsilon$, where $\Delta\epsilon$ is the total spectral range contained in the Hamiltonian. In this situation, we are not bound to use a polynomial expansion of the time evolution operator and any short-time propagator can serve the purpose.

## IV. MODEL

In order to make a thorough test and compare spectral filter methods based on the correlation function with filter diagonalization, we need to have a flexible model so that we can study various regions of the parameter space. To this end we have selected the model Hamiltonian as introduced by Wyatt [30]. The model system consists of $n_b$ bands of states, with $n_s$ states in each band. The states within each band are relatively strongly coupled, with weaker coupling between states in different bands. The zeroth-order diagonal energies were chosen to lie in the interval [0,1], so that the average spacing between successive states is $1/(n_bn_s)$. The Hamil-

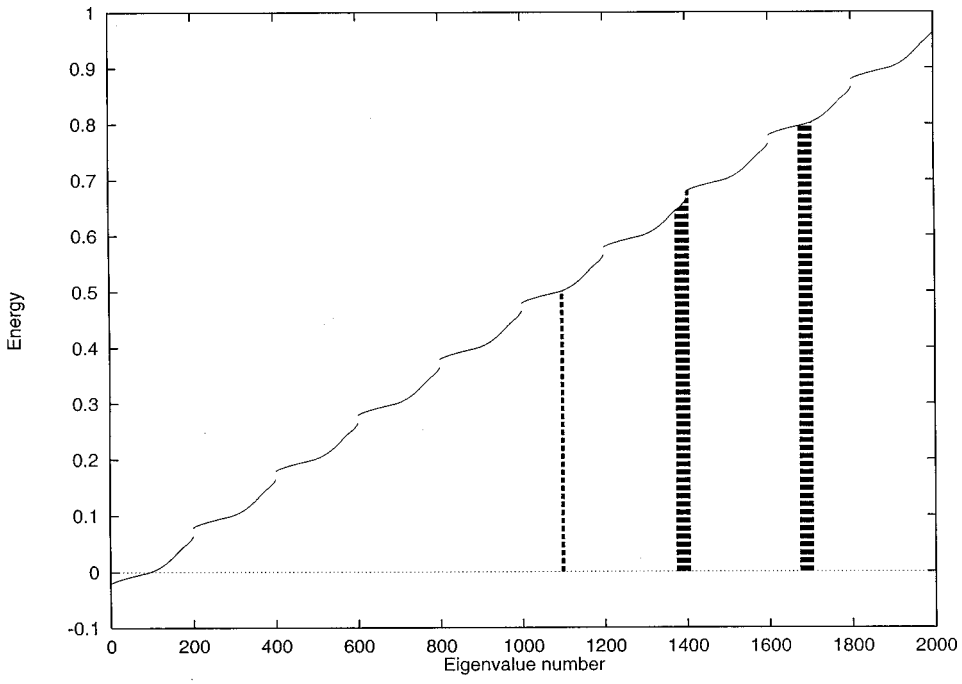


FIG. 1. The eigenvalue distribution of the model Hamiltonian. Shaded regions show the spectral windows studied here.

tonian matrix elements are specified as follows: for diagonal energies,

$$H_{ij,ij}=(i-1)\Delta+(j-1)\delta, \quad \text{where} \quad \delta \ll \Delta;$$

for intraband coupling,

$$H_{ij,ij'}=C\exp(-|j-j'|);$$

and for interband coupling,

$$H_{ij,i'j'}=[C/(n_{od}|i-i'|+1)]\exp(-|j-j'|),$$

where $i$ denotes the band index, $i=1,2,\ldots,n_b$, and $j$ denotes the index for states in this band, $j=1,2,\ldots,n_s$. As is implicit, the model consists of six parameters, in which $n_s$ determines the density of states and the parameter $n_{od}$ adjusts the interband coupling relative to the intraband coupling. In the present study, we choose the following values for the parameters: $n_b=10$, $n_s=200$, $C=0.05$, $\Delta=0.1$, $\delta=0.0001$, and $n_{od}=5$. The eigenvalue distribution for this model as obtained by exact diagonalization is shown in Fig. 1.

## V. RESULTS AND DISCUSSION

We first analyze the results obtained by the FD method. The FD method utilizes two free parameters which have to be adjusted in the numerical experiment, viz., the number of Chebyshev terms, $N$ [$2N$ in Eq. (A8)], and the number of basis functions, $L$ [Eq. (15)], in the given window. The number of Chebyshev terms required for an accurate determination of the eigenspectrum in a given window is directly related to the total propagation time, as we know that the series in Eq. (8) has exponential convergence if the order of the Bessel function is greater than its argument. In order to test the performance of the FD method, we have examined various spectral windows from different regions of the spectrum as indicated in Fig. 1, and in what follows we present some representative results. We first concentrate on the window (1095–1102), for which we compare the FD results with the

TABLE I. A comparison of exact and FD eigenvalues for the model Hamiltonian.

| No. | Exact | (8100/28)[a] | | (8100/30)[a] | | (8200/28)[a] | |
|---|---|---|---|---|---|---|---|
| 1095 | 0.500 161 66 | 0.500 161 66 | (0.052 01) | 0.500 161 66 | (0.189 94) | 0.500 161 68 | (0.146 17) |
| | | | | 0.500 330 80 | (27.330 79) | | |
| 1096 | 0.500 409 13 | 0.500 409 13 | (0.050 99) | 0.500 409 15 | (0.340 96) | 0.500 409 14 | (0.090 10) |
| 1097 | 0.500 663 68 | 0.500 663 68 | (0.010 37) | 0.500 663 68 | (0.016 83) | 0.500 663 68 | (0.013 90) |
| 1098 | 0.500 925 29 | 0.500 925 29 | (0.074 05) | 0.500 925 29 | (0.081 52) | 0.500 925 30 | (0.081 38) |
| 1099 | 0.501 193 97 | 0.501 193 97 | (0.004 84) | 0.501 193 97 | (0.004 82) | 0.501 193 97 | (0.004 79) |
| 1100 | 0.501 469 75 | 0.501 469 75 | (0.002 10) | 0.501 469 75 | (0.002 07) | 0.501 469 75 | (0.011 93) |
| | | | | | | 0.501 497 05 | (24.445 96) |
| 1101 | 0.501 752 67 | 0.501 752 67 | (0.003 57) | 0.501 752 67 | (0.003 69) | 0.501 752 67 | (0.003 65) |
| 1102 | 0.502 042 77 | 0.502 042 77 | (0.026 20) | 0.502 042 77 | (0.035 54) | 0.502 042 77 | (0.043 67) |

[a]$(N/L)$ refers to the number of Chebyshev terms and the number of filtered states. The error, $\Delta\epsilon_m\times10^3$ [Eq. (18)] is given in the parentheses.

TABLE II. A comparison of exact and FD eigenvalues as a function of relative phase for the model Hamiltonian.

| | | FD (relative phase)[a] | | | | | | |
|---|---|---|---|---|---|---|---|---|
| No. | Exact | 1.10 | 1.00 | 0.90 | 0.80 | 0.75 | 0.70 | 0.60 |
| 1095 | 0.500 161 66 | 0.500 161 44 | 0.500 147 33 | 0.500 169 79 | 0.500 209 65 | 0.500 241 78 | | |
| 1096 | 0.500 409 13 | 0.500 408 53 | 0.500 356 13 | 0.500 433 93 | 0.500 368 38 | | 0.500 313 25 | |
| 1097 | 0.500 663 68 | 0.500 663 62 | 0.500 644 84 | 0.500 666 02 | 0.500 656 66 | 0.500 659 19 | 0.500 672 93 | 0.500 611 69 |
| 1098 | 0.500 925 29 | 0.500 921 17 | 0.500 699 10 | | | | | |
| 1099 | 0.501 193 97 | 0.501 193 95 | 0.501 193 32 | 0.501 192 44 | 0.501 176 03 | 0.501 192 58 | 0.501 224 08 | 0.501 101 00 |
| 1100 | 0.501 469 75 | 0.501 469 75 | 0.501 469 63 | 0.501 469 33 | 0.501 457 38 | 0.501 471 87 | 0.501 488 79 | 0.501 457 58 |
| 1101 | 0.501 752 67 | 0.501 752 66 | 0.501 752 50 | 0.501 751 96 | 0.501 707 93 | 0.501 761 35 | 0.501 782 62 | 0.501 768 51 |
| | | 0.502 025 36 | | | | | | |
| 1102 | 0.502 042 77 | 0.502 043 06 | 0.502 041 41 | 0.502 037 81 | 0.501 876 98 | | | |

[a]The relative phase is with reference to the minimum eigenvalue gap in the window.

exact ones in Table I. This window has a total of eight eigenvalues, and with several trials we found 28 filtered states ($L=28$) to be sufficient for an accurate determination of the spectrum. With 28 filtered states, we then systematically examined the convergence of the window eigenvalues as a function of the number of Chebyshev terms ($N$) in Eq. (A8), and found that 14 400 terms ($2N$) are generally sufficient to identify the spectrum (with the correct number of eigenvalues and the error estimate being smaller than the eigenvalue gap), while 16 200 terms were necessary to obtain eight-digit accuracy with respect to eigenvalues obtained by direct diagonalization. This result gives us some insight into the convergence of the FD method, as we expect the convergence to be dictated by the local eigenvalue gap in the given window. Within this spectral window, the average $\Delta\epsilon_{\mathrm{avg}}$ (largest/smallest, $\Delta\epsilon_{\mathrm{lar}}/\Delta\epsilon_{\mathrm{sma}}$) eigenvalue gap is 0.000 268 73 (0.000 290 1/0.000 247 47), and for the present model system, the $\overline{\lambda}$ and $\Delta\lambda$ parameters are 0.472 363 615 and 0.493 222 455, respectively. Thus the 16 200 Chebyshev recursions would have been sufficient to propagate the wave packet at a time of about $T_{\mathrm{tot}}=32\,845$ units, and this corresponds to the relative phase which the levels receive within this time $[(T_{\mathrm{tot}}/2\pi)^{*}\Delta\epsilon_{\mathrm{avg/lar/sma}}]$ to be about 1.41/1.52/1.29, which is larger than one oscillation. The time-energy uncertainty principle predicts the relative phase to be larger than 1.0 for an accurate identification of eigenvalues. In Table II, we compare the FD predicted eigenvalues as a function of the relative phase (which has been computed with reference to the smallest eigenvalue gap in the window). The number of filtered states ($L$) was taken to be 50. It is clear from Table II that one has to go beyond the time-energy uncertainty regime (relative phase higher than 1.0) for a reliable prediction of eigenvalues. Thus we see that the FD method remains within the bound of the uncertainty constraint, which is contrary to earlier claims [3,20]. From Tables I and II, we also note the appearance of spurious eigenvalues when we increase the number of Chebyshev recursions, which is reminiscent of the well-known Lanczos method. However, spurious eigenvalues also appear when we change the number of filtered states ($L$) utilized in the reduced eigenvalue problem. With the FD method, these spurious eigenvalues appear to be easily identified if we set somewhat stringent criteria in the computed error norm, as is clear from Table I. We have also found that the number of filtered states ($L$) and the number of Chebyshev terms ($N$) are, in general, coupled parameters for lower values of $L$, and beyond certain $L$ the FD method is generally dependent only on $N$.

We next examine a somewhat larger spectral window in the eigenvalue range from 0.796 to 0.803 (1673–1705). This window has a total of 33 eigenstates, and 50 filtered states ($L$) were found to be sufficient for an accurate determination of eigenvalues. Within this window, the average $\Delta\epsilon_{\mathrm{avg}}$ (largest/smallest, $\Delta\epsilon_{\mathrm{lar}}/\Delta\epsilon_{\mathrm{sma}}$) eigenvalue gap is 0.000 216 17 (0.000 312 82/0.000 168 09), and 6500 Chebyshev terms ($2N=13\,000$) were found to be sufficient for convergence of the eigenvalues. In Table III, we compare the FD result for this window with the exact ones (the results with 7000 terms are shown to highlight the appearance of spurious eigenvalues). We immediately see that the total relative phase which the levels receive here is about 0.91, 0.71, and 1.31 when compared to the average, smallest, and the largest level spacing, respectively, in the window. Thus the performance of the FD method in this case seems to hover around the time-energy uncertainty regime and it is apparently difficult to claim whether or not we have really been able to bypass the uncertainty constraint in any significant way.

We finally examine the window in the eigenvalue range from 0.644 to 0.682 (1374–1407) in Table IV. The feature of this window is qualitatively different from the previous windows; that is, the level spacing differs significantly in different regions of the spectrum (the average, smallest, and the largest level gap being 0.001 139 31, 0.000 349 66, and 0.014 697 45, respectively). The number of filtered states required for a faithful reproduction of the eigenvalues is $L=100$ as compared to 50 in the previous window (1673–1705), in spite of the fact that the number of states in both the windows is almost the same. With 7000 Chebyshev terms required in this case, the relative phase which the levels receive is found to be about 2.57, 0.79, and 33.20, respectively, when compared to the average, smallest, and the largest level spacing in the window. Thus the examples shown here clearly indicate that the behavior of the FD method is solely guided by the local eigenvalue gap structure in the given window, and with reference to the smallest level gap, the method may sometimes seem to bypass the uncertainty constraint. Hence we conclude that the time-energy uncertainty is lurking here in a somewhat indirect manner, and the

TABLE III. A comparison of exact and FD eigenvalues for the model Hamiltonian.

| No. | Exact | (700/50)[a] | |
|---|---|---|---|
| 1673 | 0.796 075 29 | 0.796 075 20 | (0.315 51) |
| 1674 | 0.796 248 08 | 0.796 247 94 | (0.422 59) |
| 1675 | 0.796 420 28 | 0.796 420 26 | (0.153 23) |
| 1676 | 0.796 591 88 | 0.796 591 88 | (0.048 72) |
| 1677 | 0.796 762 90 | 0.796 762 90 | (0.019 08) |
| 1678 | 0.796 933 36 | 0.796 933 36 | (0.020 86) |
| 1679 | 0.797 103 26 | 0.797 103 25 | (0.046 99) |
| 1680 | 0.797 272 60 | 0.797 272 60 | (0.015 04) |
| 1681 | 0.797 441 42 | 0.797 441 42 | (0.007 36) |
| 1682 | 0.797 609 77 | 0.797 609 77 | (0.009 54) |
| 1683 | 0.797 777 86 | 0.797 777 86 | (0.008 77) |
| 1684 | 0.797 946 31 | 0.797 946 31 | (0.010 13) |
| 1685 | 0.798 116 53 | 0.798 116 53 | (0.016 55) |
| 1686 | 0.798 290 68 | 0.798 290 68 | (0.004 45) |
| 1687 | 0.798 470 94 | 0.798 470 94 | (0.003 19) |
| 1688 | 0.798 658 69 | 0.798 658 69 | (0.001 33) |
| 1689 | 0.798 854 44 | 0.798 854 44 | (0.002 37) |
| 1690 | 0.799 058 20 | 0.799 058 20 | (0.127 83) |
| | | 0.799 094 78 | (34.964 31) |
| 1691 | 0.799 269 77 | 0.799 269 77 | (0.001 95) |
| 1692 | 0.799 488 93 | 0.799 488 93 | (0.000 30) |
| 1693 | 0.799 715 49 | 0.799 715 49 | (0.000 33) |
| 1694 | 0.799 949 33 | 0.799 949 33 | (0.001 14) |
| 1695 | 0.800 190 34 | 0.800 190 34 | (0.000 65) |
| 1696 | 0.800 438 47 | 0.800 438 47 | (0.000 87) |
| 1697 | 0.800 693 68 | 0.800 693 68 | (0.000 09) |
| 1698 | 0.800 955 98 | 0.800 955 98 | (0.000 42) |
| 1699 | 0.801 225 36 | 0.801 225 36 | (0.000 65) |
| 1700 | 0.801 501 86 | 0.801 501 86 | (0.000 45) |
| 1701 | 0.801 785 50 | 0.801 785 50 | (0.000 81) |
| 1702 | 0.802 076 35 | 0.802 076 35 | (0.000 33) |
| 1703 | 0.802 374 46 | 0.802 374 46 | (0.000 78) |
| 1704 | 0.802 679 89 | 0.802 679 89 | (0.000 16) |
| 1705 | 0.802 992 71 | 0.802 992 71 | (0.002 11) |

[a]$(N/L)$ refers to the number of Chebyshev terms and the number of filtered states. The error $\Delta\epsilon_m \times 10^3$ [Eq. (18)] is given in the parentheses.

general claim of the FD method going beyond the uncertainty regime may be rather fortuitous.

We now turn to the correlation function realization of the spectral filter method, and our objective is to evaluate the number of propagation steps needed for a reliable identification of the spectrum. We recall that the accurate reproduction of eigenvalues here would involve the location of zeros of the first derivative of the correlation function, along with knowledge of the second derivative, and for this we can employ any appropriate method, for example the Newton-Raphson method. Features of the correlation function itself will give sufficient insight into the problem. As an example, we have selected the window with eigenvalues ranging from 0.796 to 0.803 for comparison with the FD method. For this window, the FD method required about 13 000 Chebyshev terms for the determination of eigenvalues. We have employed the same number of Chebyshev terms in Eq. (11) and scanned the correlation amplitude as a function of energy, which is plotted in Fig. 2. Also shown in Fig. 2 are plots of the first and the second derivatives of the correlation amplitude [Eqs. (12) and (13)], which have been scaled arbitrarily. This window has 33 eigenvalues and we can immediately see that the correlation function does have 33 peaks. In fact, the first and the second derivatives of the correlation amplitude in Fig. 2 show 35 peaks, of which two peaks have vanishingly small intensities and hence they are spurious. The appearance of spurious eigenvalues is thus seen as a common feature for both FD and correlation function methods. In the limit of infinite time propagation, we would expect 33 $\delta$ peaks and the peak height would correspond to the signal intensity. Thus we see that the total time propagation required for the identification of the spectrum by the correlation function method is similar to the one in the FD method. The essential difference now is in the exact location of the eigenvalue, for which the correlation function method has to rely on our ability to exactly locate the zeros of the first derivative (in principle, there is no fundamental problem), whereas the FD method implements matrix diagonalization for this purpose.

We finally make some remarks on the computation of the spectral intensity, $A_m = \langle \phi(x,\epsilon_m) | \psi(x,0) \rangle$ [Eq. (1)]. This computation requires that Eq. (11) be properly normalized. As in the practical calculation, we employ only a finite number of Chebyshev terms and this essentially amounts to finite-time propagation. Then we can utilize $1/\sqrt{2T}$ normalization in Eq. (6) and estimate $T$ from the argument of the Bessel function in Eq. (8). Computation of spectral intensities by the FD method is also straightforward and it has been discussed in detail in the literature [19,27,34].

## VI. CONCLUSION

We have demonstrated in this study that the time-domain theory of spectral filters may be viewed as originating from the notion of *selective measurement* in quantum mechanics, and different filter algorithms differ essentially in the way we approximate the measurement operator, which is the $\delta$-function operator. We have further shown that a *legitimate* integral representation of the measurement operator is possible with the help of the Fourier integral theorem, and this unifying theme has helped us to clarify the role of the time-energy uncertainty principle to the numerical performance of the filter operator, which has been implemented here in the continuous correlation function as well as in the FD form. The continuous correlation function and the FD methods both utilize equivalent propagation times and they differ only in the algorithm used to locate the eigenvalues. From practical considerations, the diagonalization step in the FD method appears to be more convenient than the location of zeros in the correlation function method. Thus we do not verify the commonly held notion that the FD method can bypass the time-energy uncertainty constraint. Numerical experiments have shown the FD method to share some features with the well-known Lanczos reduction technique.

## ACKNOWLEDGMENTS

This work was supported in part by the Natural Science Foundation and the Robert Welch Foundation.

TABLE IV. A comparison of exact and FD eigenvalues for the model Hamiltonian.

| No. | Exact | (3500/100)[a] | | (3500/50)[a] | |
|---|---|---|---|---|---|
| 1374 | 0.644 211 66 | 0.644 211 66 | (0.015 74) | 0.644 199 66 | (0.873 86) |
| 1375 | 0.644 892 39 | 0.644 892 39 | (0.000 82) | 0.644 877 28 | (2.021 75) |
| 1376 | 0.645 551 00 | 0.645 551 00 | (0.000 14) | 0.645 857 67 | (8.010 61) |
| 1377 | 0.646 184 81 | 0.646 184 81 | (0.000 02) | | |
| 1378 | 0.646 793 16 | 0.646 793 16 | (0.000 03) | 0.646 716 34 | (5.687 86) |
| 1379 | 0.647 380 35 | 0.647 380 35 | (0.000 07) | 0.647 152 32 | (9.983 40) |
| | | | | 0.647 712 86 | (10.135 01) |
| 1380 | 0.647 956 80 | 0.647 956 80 | (0.000 08) | 0.648 061 53 | (6.111 86) |
| 1381 | 0.648 534 36 | 0.648 534 36 | (0.000 07) | | |
| 1382 | 0.649 120 70 | 0.649 120 70 | (0.000 09) | 0.649 119 64 | (0.432 36) |
| 1383 | 0.649 719 16 | 0.649 719 16 | (0.000 12) | 0.649 715 88 | (1.035 55) |
| 1384 | 0.650 331 27 | 0.650 331 27 | (0.000 09) | 0.650 328 80 | (1.051 41) |
| 1385 | 0.650 958 16 | 0.650 958 16 | (0.000 09) | 0.650 954 92 | (1.361 04) |
| 1386 | 0.651 601 07 | 0.651 601 07 | (0.000 10) | 0.651 582 10 | (2.279 36) |
| 1387 | 0.652 261 38 | 0.652 261 38 | (0.000 12) | 0.652 260 22 | (0.957 25) |
| 1388 | 0.652 940 73 | 0.652 940 73 | (0.000 08) | 0.652 940 42 | (0.551 02) |
| 1389 | 0.653 641 06 | 0.653 641 06 | (0.000 05) | 0.653 640 97 | (0.325 83) |
| 1390 | 0.654 364 70 | 0.654 364 70 | (0.000 07) | 0.654 364 65 | (0.273 75) |
| 1391 | 0.655 114 47 | 0.655 114 47 | (0.000 09) | 0.655 114 44 | (0.211 77) |
| | | | | 0.655 591 57 | (72.278 46) |
| 1392 | 0.655 893 88 | 0.655 893 88 | (0.000 05) | 0.655 893 88 | (0.060 85) |
| 1393 | 0.656 707 42 | 0.656 707 42 | (0.000 11) | 0.656 707 42 | (0.053 00) |
| 1394 | 0.657 560 92 | 0.657 560 92 | (0.000 05) | 0.657 560 92 | (0.023 27) |
| 1395 | 0.658 462 27 | 0.658 462 27 | (0.000 01) | 0.658 462 27 | (0.058 01) |
| 1396 | 0.659 422 69 | 0.659 422 69 | (0.000 07) | 0.659 422 69 | (0.001 53) |
| 1397 | 0.660 459 12 | 0.660 459 12 | (0.000 03) | 0.660 459 12 | (0.000 56) |
| 1398 | 0.661 599 69 | 0.661 599 69 | (0.000 08) | 0.661 599 69 | (0.000 32) |
| 1399 | 0.662 898 73 | 0.662 898 73 | (0.000 07) | 0.662 898 73 | (0.000 21) |
| 1400 | 0.664 497 63 | 0.664 497 63 | (0.000 05) | 0.664 497 63 | (0.000 27) |
| 1401 | 0.679 195 08 | 0.679 195 08 | (0.000 47) | 0.679 195 09 | (0.025 54) |
| 1402 | 0.679 782 14 | 0.679 782 14 | (0.002 27) | 0.679 815 27 | (2.683 79) |
| 1403 | 0.680 265 78 | 0.680 265 78 | (0.000 66) | 0.680 266 06 | (0.218 27) |
| 1404 | 0.680 695 43 | 0.680 701 61 | (0.753 84) | | |
| 1405 | 0.681 090 00 | 0.681 090 03 | (0.051 87) | | |
| 1406 | 0.681 459 19 | 0.681 459 21 | (0.041 00) | 0.681 384 89 | (2.854 27) |
| 1407 | 0.681 808 85 | 0.681 808 88 | (0.126 93) | 0.681 740 35 | (4.280 40) |

[a]$(N/L)$ refers to the number of Chebyshev terms and the number of filtered states. The error $\Delta\epsilon_m\times 10^3$ [Eq. (18)] is given in the parentheses.

## APPENDIX A: MATRIX ELEMENTS FOR CONTINUOUS-TIME FD

Here we present a derivation of the overlap, Hamiltonian, and error matrix elements [Eqs. (16), (17), and (19)] with respect to the filtered states, Eq. (14). Since $\hat{\mathcal{H}}=\Delta\lambda\overline{H}+\overline{\lambda}$, the required matrix elements can be written as follows:

$$S_{mn}=\langle\chi(x,E_m)|\chi(x,E_n)\rangle, \tag{A1}$$

$$H_{mn}=\Delta\lambda\langle\chi(x,E_m)|\overline{H}|\chi(x,E_n)\rangle+\overline{\lambda}S_{mn}, \tag{A2}$$

$$H^2_{mn}=(\Delta\lambda)^2\langle\chi(x,E_m)|(\overline{H})^2|\chi(x,E_n)\rangle+2\overline{\lambda}H_{mn}-(\overline{\lambda})^2S_{mn}. \tag{A3}$$

In the following, we evaluate the general matrix element, $R^p_{mn}=\langle\chi(x,E_m)|(\overline{H})^p|\chi(x,E_n)\rangle$, from which we can recover the individual matrix elements, $S_{mn}$, $H_{mn}$, and $H^2_{mn}$ by specializing with $p=0$, 1, and 2, respectively. Taking Eq. (10) as the representation of the projection operator required in Eq. (14), we have the following expression for the filtered states:

$$|\chi(x,E_m)\rangle=\frac{4}{\Delta\lambda}\sum_{k=0}^{N\to\infty}\left(1-\frac{\delta_{k0}}{2}\right)\frac{\cos k\theta_m}{\sin\theta_m}T_k(\overline{H})|\psi(x,0)\rangle, \tag{A4}$$

where $\cos\theta_m=\overline{E_m}$. Thus the matrix element $R^p_{mn}$ can be written as follows:

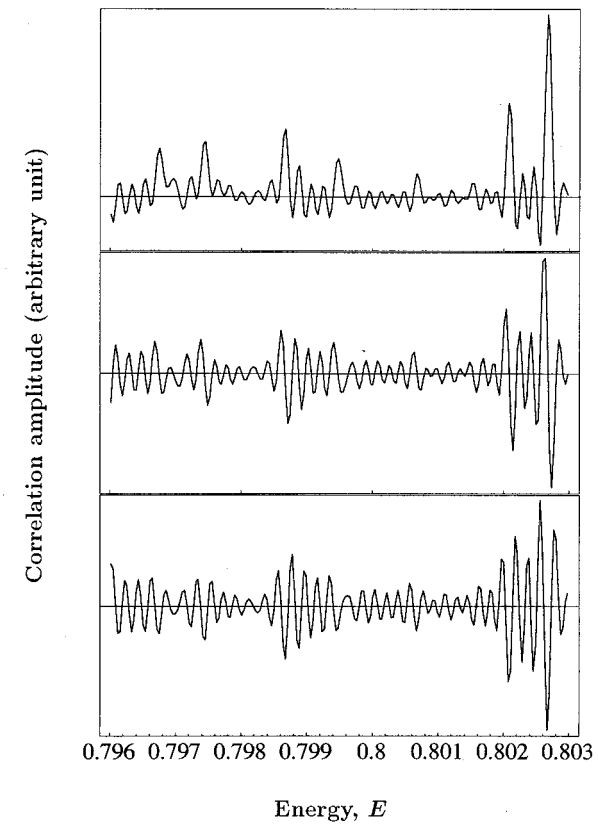


FIG. 2. The correlation amplitude (top panel) and its first (central panel) and second derivative (bottom panel) as a function of energy. The intensity is plotted in arbitrary units.

$$R^p_{mn}=\langle\chi(x,E_m)|(\bar{H})^p|\chi(x,E_n)\rangle$$
$$=\frac{16}{(\Delta\lambda)^2}\sum_{k=0}^{N\to\infty}\sum_{k'=0}^{N\to\infty}\left(1-\frac{\delta_{k0}}{2}\right)$$
$$\times\left(1-\frac{\delta_{k'0}}{2}\right)\frac{\cos k\theta_m\cos k'\theta_n}{\sin\theta_m\sin\theta_n}$$
$$\times\langle\psi(x,0)|T_k(\bar{H})T_{k'}(\bar{H})[T_1(\bar{H})]^p|\psi(x,0)\rangle. \tag{A5}$$

By utilizing the property of Chebyshev polynomials, $2T_k(\bar{H})T_{k'}(\bar{H})=T_{k+k'}(\bar{H})+T_{k-k'}(\bar{H})$, it is straightforward to show that

$$T_k(\bar{H})T_{k'}(\bar{H})[T_1(\bar{H})]^p=\tfrac{1}{2}[U^p_{k+k'}(\bar{H})+U^p_{k-k'}(\bar{H})] \tag{A6}$$

with $2U^p_k(\bar{H})=[T_{k+p}(\bar{H})+T_{k-p}(\bar{H})]$. Thus Eq. (A5) can be written as

$$R^p_{mn}=\frac{4}{(\Delta\lambda)^2}\sum_{k=0}^{N\to\infty}\sum_{k'=0}^{N\to\infty}\left(1-\frac{\delta_{k0}}{2}\right)\left(1-\frac{\delta_{k'0}}{2}\right)$$
$$\times\frac{2\cos k\theta_m\cos k'\theta_n}{\sin\theta_m\sin\theta_n}(c^p_{k+k'}+c^p_{k-k'}) \tag{A7}$$

with $c^p_k=\langle\chi(x,E_m)|U^p_k(\bar{H})|\chi(x,E_n)\rangle$. The double summation in Eq. (A7) can be further simplified as shown by Mandelshtam and Taylor [19]. Before we proceed, we first note that the right-hand side of Eq. (A7) is not a finite sum, but a short-hand way of writing a complicated double limit. Since the addition is a step-by-step process, the quantities to be added must first be arranged in a sequence and there is no unique rule for selecting the order in which they are to be taken. It is well known that the limit of the sum of terms of a conditionally convergent series may depend upon the order in which the terms are taken but that the terms of an absolutely convergent series can be arranged arbitrarily. Assuming the absolute convergence of series (A4), we can employ a *Cauchy-like expansion* [47] of the product of two series [Eq. (A7)] and this allows us to rearrange the terms in the product in such a way that all the terms for which $(k+k')$ and $(k-k')$ have the same values, are grouped together, and then perform the summation (this is also called the diagonal summation of the double series). Thus we obtain

$$R^p_{mn}=\frac{4}{(\Delta\lambda)^2}\frac{1}{\sin\theta_m\sin\theta_n}$$
$$\times\left[A_0C_0+\sum_{l=1}^{N}A_lC_l+\sum_{l=0}^{N-1}A_{2N-l}C_{2N-l}\right] \tag{A8}$$

with

$$A_{2N-l}=\sum_{r=0}^{l}2\cos(N-r)\theta_m\cos(N-l+r)\theta_n, \tag{A9}$$

$$A_l=\left\{\sum_{r=0}^{l}2\cos r\theta_m\cos(l-r)\theta_n-(\cos l\theta_m+\cos l\theta_n)\right\}$$
$$+\left\{\sum_{r=0}^{N-l}2\cos(N-r)\theta_m\cos(N-l-r)\theta_n-\cos l\theta_m\right\}$$
$$+\left\{\sum_{r=0}^{N-l}2\cos(N-l-r)\theta_m\cos(N-r)\theta_n-\cos l\theta_n\right\}, \tag{A10}$$

$$A_0=\left\{\sum_{r=0}^{N}2\cos r\theta_m\cos r\theta_n\right\}-1. \tag{A11}$$

In Eqs. (A10) and (A11), negative terms appear due to the consideration of the $\delta$ function in Eq. (A7). The summation in Eqs. (A9)–(A11) can now be carried out analytically. We first consider the diagonal terms $(m=n)$. Equation (A9) can be rewritten as follows:

$$A_{2N-l}=\sum_{r=0}^{l}\{\cos(2N-l)\theta_m+\cos(2r-l)\theta_m\}$$
$$=(l+1)\cos(2N-l)\theta_m+\sum_{r=0}^{l}\cos(2r-l)\theta_m. \tag{A12}$$

The summation in Eq. (A12) can be easily obtained by recognizing this as the real part of $\Sigma_{r=0}^{l}\exp[i(2r-l)\theta_m]$, which is a geometrical series and can be summed by the standard formulas. We now change the variable, $2N-l=s$, and thus obtain

$$A_s=(2N-s+1)\cos s\theta_m + \frac{\sin(2N-s+1)\theta_m}{\sin\theta_m} \quad (N+1\leqslant s\leqslant 2N). \quad \text{(A13)}$$

Following the similar procedure, it can easily be shown that the explicit summation in Eq. (A10) results in an expression exactly similar to Eq. (13), whereas Eq. (A11) gives rise to one-half of an expression similar to Eq. (13). Therefore, Eq. (A8) for diagonal terms can be rearranged as follows:

$$R^p_{mm}=\frac{4}{(\Delta\lambda)^2}\frac{1}{\sin^2\theta_m}\sum_{k=0}^{2N}\left(1-\frac{\delta_{k0}}{2}\right)c_k^p \times\left[(2N-k+1)\cos k\theta_m+\frac{\sin(2N-k+1)\theta_m}{\sin\theta_m}\right]. \quad \text{(A14)}$$

We now proceed to evaluate the off-diagonal terms. For $m\neq n$, Eq. (A9) can be rewritten as follows:

$$\begin{aligned}A_{2N-l}&=\sum_{r=0}^{l}2\cos(N-r)\theta_m\cos(N-l+r)\theta_n \times\left(\frac{\cos\theta_m-\cos\theta_n}{\cos\theta_m-\cos\theta_n}\right)\\ &=\frac{1}{\cos\theta_m-\cos\theta_n}\times\left\{\sum_{r=0}^{l}\cos(N-r+1)\theta_m\cos(N-l+r)\theta_n\right.\\ &\quad+\sum_{r=0}^{l}\cos(N-r-1)\theta_m\cos(N-l+r)\theta_n\\ &\quad-\sum_{r=0}^{l}\cos(N-r)\theta_m\cos(N-l+r+1)\theta_n\\ &\quad\left.-\sum_{r=0}^{l}\cos(N-r)\theta_m\cos(N-l+r-1)\theta_n\right\}. \quad \text{(A15)}\end{aligned}$$

We now pull out $r=0$ terms from the first and the last summation, and $r=l$ terms from the second and the third summation in Eq. (A15), to find that the remaining terms identically cancel. On substituting $s=2N-l(N+1\leqslant s\leqslant 2N$ as $0\leqslant l\leqslant N-1)$, we thus obtain

$$\begin{aligned}A_s&=\cos(N+1)\theta_m\cos(N-s)\theta_n-\cos N\theta_m\cos(N-s+1)\theta_n\\ &\quad-\cos(N+1)\theta_n\cos(N-s)\theta_m\\ &\quad+\cos N\theta_n\cos(N-s+1)\theta_m. \quad \text{(A16)}\end{aligned}$$

Following a similar procedure, it can easily be shown that the summation in Eq. (A10) gives rise to expressions similar to Eq. (A16), whereas Eq. (A11) results in one-half of the expressions similar to Eq. (A16). Therefore, Eq. (A8) for off-diagonal terms can be rearranged to the following result:

$$\begin{aligned}R^p_{mn}&=\frac{4}{(\Delta\lambda)^2}\frac{1}{(\cos\theta_m-\cos\theta_n)}\\ &\quad\times\left[\frac{\cos(N+1)\theta_m}{\sin\theta_m}\sum_{k=0}^{2N}\left(1-\frac{\delta_{k0}}{2}\right)c_k^p\frac{\cos(N-k)\theta_n}{\sin\theta_n}\right.\\ &\quad-\frac{\cos N\theta_m}{\sin\theta_m}\sum_{k=0}^{2N}\left(1-\frac{\delta_{k0}}{2}\right)c_k^p\frac{\cos(N-k+1)\theta_n}{\sin\theta_n}\\ &\quad-\frac{\cos(N+1)\theta_n}{\sin\theta_n}\sum_{k=0}^{2N}\left(1-\frac{\delta_{k0}}{2}\right)c_k^p\frac{\cos(N-k)\theta_m}{\sin\theta_m}\\ &\quad\left.+\frac{\cos N\theta_n}{\sin\theta_n}\sum_{k=0}^{2N}\left(1-\frac{\delta_{k0}}{2}\right)c_k^p\frac{\cos(N-k+1)\theta_m}{\sin\theta_m}\right]\\ &\quad(m\neq n). \quad \text{(A17)}\end{aligned}$$

To make passage from Eq. (A7) to Eqs. (A14) and (A17), we have assumed that the filtered states obtained by truncating the series in Eq. (A4) at $N$ are sufficient to form a basis to yield correct eigenvalues in the given window, by conventional matrix diagonalization.

## APPENDIX B: MATRIX ELEMENTS FOR DISCRETE-TIME FD

Here we present a discrete-time implementation of the FD method, in the spirit of Ref. [19]. Let us first consider the eigenvalue problem:

$$\hat{\mathcal{H}}|\phi(x,\epsilon_m)\rangle=\epsilon_m|\phi(x,\epsilon_m)\rangle. \quad \text{(B1)}$$

It is easy to show by induction that Eq. (B1) also implies

$$f(\hat{\mathcal{H}})|\phi(x,\epsilon_m)\rangle=f(\epsilon_m)|\phi(x,\epsilon_m)\rangle, \quad \text{(B2)}$$

where $f(\hat{\mathcal{H}})$ is a rational function of the form $p(\hat{\mathcal{H}})^{-1}q(\hat{\mathcal{H}})$, where $p(\hat{\mathcal{H}})$ and $q(\hat{\mathcal{H}})$ are either polynomials or transcendental functions with convergent power series expansion. As explained in Appendix A, Eq. (B2) demands us to consider the general matrix element, $R^p_{mn}=\langle\chi(x,E_m)|[f(\hat{\mathcal{H}})]^p|\chi(x,E_n)\rangle$. As shown in Ref. [19], it is convenient to take $e^{-i\hat{\mathcal{H}}\Delta t}$ for $f(\hat{\mathcal{H}})\,(=\hat{R})$ in Eq. (B2), in order to simplify the expression for the overlap and the Hamiltonian matrices. Next we consider the discretization of Eq. (14) in the following form:

$$\begin{aligned}|\chi(x,E_m)\rangle&=\lim_{T\to\infty}\int_{-T}^{T}dt\,e^{iE_mt}e^{-i\hat{\mathcal{H}}t}|\psi(x,0)\rangle\\ &=\sum_{k=0}^{N\to\infty}e^{i(E_m\Delta t)k}e^{-i(\hat{\mathcal{H}}\Delta t)k}|\psi(x,0)\rangle\\ &=\sum_{k=0}^{N\to\infty}(\hat{R}/Z_m)^k|\psi(x,0)\rangle, \quad \text{(B3)}\end{aligned}$$

where $Z_m=e^{-i(E_m\Delta t)k}$. With Eq. (B3), the general matrix element takes the following form:

$$R^p_{mn}=\langle\chi(x,E_m)|\hat{R}^p|\chi(x,E_n)\rangle$$
$$=\sum_{k=0}^{N}\sum_{k'=0}^{N} Z_m^{-k}Z_n^{-k'}(\hat{R}^k\psi(x,0)|\hat{R}^p|\hat{R}^{k'}\psi(x,0))$$
$$=\sum_{k=0}^{N}\sum_{k'=0}^{N} Z_m^{-k}Z_n^{-k'}(\psi(x,0)|\hat{R}^{k+k'+p}|\psi(x,0))$$
$$=\sum_{k=0}^{N}\sum_{k'=0}^{N} c_{k+k'+p}Z_m^{-(k+k')}\left(\frac{Z_m}{Z_n}\right)^{k'}. \quad \text{(B4)}$$

In Eq. (B4), we have introduced a complex symmetric inner product (i.e., no complex conjugation), which is appropriate when complex symmetric operators are involved [48]. As discussed in Appendix A, we can now carry out a *Cauchy-like expansion* [47] of the double series in Eq. (B4) and perform the partial summation. Off-diagonal elements take the following form:

$$R^p_{mn}=\sum_{l=0}^{N} c_{l+p}Z_m^{-l}\left[\sum_{k'=0}^{l}\left(\frac{Z_m}{Z_n}\right)^{k'}\right]$$
$$+\sum_{l=N+1}^{2N} c_{l+p}Z_m^{-N}Z_n^{N-l}\left[\sum_{k'=0}^{2N-l}\left(\frac{Z_m}{Z_n}\right)^{k'}\right]. \quad \text{(B5)}$$

The quantity within the square brackets in Eq. (B5), is often called the convolution of the original series. After summing the geometrical series in Eq. (B5), we finally obtain the following expression for off-diagonal ($m\neq n$) elements:

$$R^p_{mn}=\frac{1}{(Z_m-Z_n)}\left[\left(Z_m\sum_{l=0}^{N} c_{l+p}Z_n^{-l}\right)-\left(Z_n\sum_{l=0}^{N} c_{l+p}Z_m^{-l}\right)\right.$$
$$-\left(Z_m^{-N}\sum_{l=N+1}^{2N} c_{l+p}Z_n^{N-l+1}\right)$$
$$\left.+\left(Z_n^{-N}\sum_{l=N+1}^{2N} c_{l+p}Z_m^{N-l+1}\right)\right]. \quad \text{(B6)}$$

Similarly, we have the following expression for the diagonal elements:

$$R^p_{mm}=\sum_{l=0}^{N} c_{l+p}Z_m^{-l}\left(\sum_{k'=0}^{l}1\right)+\sum_{l=N+1}^{2N} c_{l+p}Z_m^{-l}\left(\sum_{k'=0}^{2N-l}1\right)$$
$$=\sum_{l=0}^{N} c_{l+p}Z_m^{-l}(l+1)+\sum_{l=N+1}^{2N} c_{l+p}Z_m^{-l}(2N-l+1)$$
$$=\sum_{l=0}^{2N} c_{l+p}Z_m^{-l}(N-|N-l|+1). \quad \text{(B7)}$$


[1] M. Blanco and E. J. Heller, J. Chem. Phys. **83**, 1149 (1985).
[2] J. H. Frederick and E. J. Heller, J. Chem. Phys. **87**, 6592 (1987).
[3] D. Neuhauser, J. Chem. Phys. **93**, 2611 (1990).
[4] D. Neuhauser, J. Chem. Phys. **95**, 4927 (1991).
[5] D. Neuhauser, J. Chem. Phys. **100**, 5076 (1994).
[6] M. R. Wall and D. Neuhauser, J. Chem. Phys. **102**, 8011 (1995).
[7] E. Narevicius, D. Neuhauser, H. J. Korsch, and N. Moiseyev, Chem. Phys. Lett. **276**, 250 (1997).
[8] G-J. Kroes, M. R. Wall, J. W. Pang, and D. Neuhauser, J. Chem. Phys. **106**, 1800 (1997).
[9] J. W. Pang, T. Dieckmann, J. Feigon, and D. Neuhauser, J. Chem. Phys. **108**, 8360 (1998).
[10] D. A. McCormack, G.-J. Kroes, and D. Neuhauser, J. Chem. Phys. **109**, 5177 (1998).
[11] Y. Huang, W. Zhu, D. J. Kouri, and D. K. Hoffman, Chem. Phys. Lett. **214**, 451 (1993).
[12] W. Zhu, Y. Huang, D. J. Kouri, C. Chandler, and D. K. Hoffman, Chem. Phys. Lett. **217**, 73 (1994).
[13] G. A. Parker, W. Zhu, Y. Huang, D. K. Hoffman, and D. J. Kouri, Comput. Phys. Commun. **96**, 27 (1996).
[14] H. Kono, Chem. Phys. Lett. **214**, 137 (1993).
[15] Y. Wang, T. Carrington, Jr., and G. C. Corey, Chem. Phys. Lett. **228**, 144 (1994).
[16] V. A. Mandelshtam and H. S. Taylor, J. Chem. Phys. **103**, 7990 (1995).
[17] V. A. Mandelshtam and H. S. Taylor, J. Chem. Phys. **103**, 10074 (1995).
[18] V. A. Mandelshtam and H. S. Taylor, J. Chem. Phys. **106**, 5085 (1997).
[19] V. A. Mandelshtam and H. S. Taylor, J. Chem. Phys. **107**, 6756 (1997).
[20] J. Main, V. A. Mandelshtam, and H. S. Taylor, Phys. Rev. Lett. **78**, 4351 (1997).
[21] V. A. Mandelshtam and H. S. Taylor, J. Chem. Phys. **108**, 9970 (1998).
[22] R. F. Salzgeber, V. A. Mandelshtam, Ch. Schlier, and H. S. Taylor, J. Chem. Phys. **110**, 3756 (1999).
[23] R. Chen and H. Guo, J. Chem. Phys. **105**, 1311 (1996).
[24] R. Chen and H. Guo, J. Comput. Phys. **136**, 494 (1997).
[25] R. Chen and H. Guo, J. Chem. Phys. **108**, 6068 (1998).
[26] R. Chen, H. Guo, L. Liu, and J. T. Muckerman, J. Chem. Phys. **109**, 7128 (1998).
[27] M. H. Beck and H.-D. Meyer, J. Chem. Phys. **109**, 3730 (1998).
[28] T. Ericsson and A. Ruhe, Math. Comput. **35**, 1251 (1980).
[29] F. Webster, P. J. Rossky, and R. A. Friesner, Comput. Phys. Commun. **63**, 494 (1991).
[30] R. E. Wyatt, Phys. Rev. E **51**, 3643 (1995).
[31] R. E. Wyatt, J. Chem. Phys. **103**, 8433 (1995).
[32] A. Maynard, R. E. Wyatt, and C. Iung, J. Chem. Phys. **106**, 9483 (1997).
[33] T. J. Minehardt, J. D. Adcock, and R. E. Wyatt, Phys. Rev. E **56**, 4837 (1997).
[34] A. Vijay, R. E. Wyatt, and G. D. Billing, J. Chem. Phys. **111**, 10 794 (1999).
[35] M. D. Feit, J. A. Fleck, Jr., and A. Steiger, J. Comput. Phys. **47**, 412 (1982).

[36] P. L. Butzer and R. L. Stens, SIAM Rev. **34**, 40 (1992), and references therein.
[37] P. A. M. Dirac, *The Principles of Quantum Mechanics* (Oxford University Press, Oxford, 1958), pp. 34–48.
[38] J. Schwinger, *Quantum Kinematics and Dynamics* (W. A. Benjamin, New York, 1970).
[39] K. Gottfried, *Quantum Mechanics* (W. A. Benjamin, New York, 1966), pp. 191–213.
[40] R. Kosloff, Annu. Rev. Phys. Chem. **45**, 145 (1994), and references therein.
[41] C. Lanczos, *Discourse on Fourier Series* (Oliver & Boyd, London, 1966).
[42] E. P. Wigner, *Group Theory* (Academic, New York, 1959), pp. 325–348.
[43] Y. Aharonov and D. Bohm, Phys. Rev. **122**, 1649 (1961), and references therein.
[44] W. H. Press, S. A. Teukolsky, W. T. Vetterling, and B. P. Flannery, *Numerical Recipe in Fortran, The Art of Scientific Computing*, 2nd ed. (Cambridge University Press, Cambridge, England, 1992), pp. 355–360.
[45] A. Szabo and N. S. Ostlund, *Modern Quantum Chemistry, Introduction to Advanced Electronic Structure Theory*, 1st ed. (McGraw-Hill, New York, 1982), pp. 142–145.
[46] L. Pauling and E. Bright Wilson, Jr., *Introduction to Quantum Mechanics With Applications to Chemistry* (Dover, New York, 1985), pp. 189 and 190.
[47] G. H. Hardy, *Divergent Series* (Clarendon, Oxford, 1949), pp. 227–230.
[48] N. Moiseyev, P. R. Certain, and F. Weinhold, Mol. Phys. **36**, 1613 (1978).